Model for Dissipative Highly Nonlinear Waves in Dry Granular Systems

Lautaro Vergara*

Departamento de Física, Universidad de Santiago de Chile, USACH, Casilla 307, Santiago 2, Chile

(Received 8 October 2009; published 16 March 2010)

A model is presented for the characterization of dissipative effects on highly nonlinear waves in one-dimensional dry granular media. The model includes three terms: Hertzian, viscoelastic, and a term proportional to the square of the relative velocity of particles. The model outcomes are confronted with different experiments where the granular system is subject to several constraints for different materials. Excellent qualitative and quantitative agreement between theory and experiments is found.

DOI: 10.1103/PhysRevLett.104.118001 PACS numbers: 45.70.−n, 05.45.Yv, 46.35.+z, 46.40.Cd

There exist a considerable number of engineering applications where surfaces are subjected to contact loading, with stress applied over small areas. Nevertheless, it is a complex matter to understand the nature of the contact of solid surfaces. A first step towards this understanding started with the work by Hertz [1]. Using potential theory, he developed a model for the normal contact on nonconforming bodies of elliptical shapes, under several assumptions that simplified the problem. One of the hypotheses on which his work was based is that the contact between solids is purely elastic.

A place where Hertz theory finds application is in the study of granular matter. This kind of matter is present everywhere in nature and has wide practical importance (see, e.g., [2]). Hertz theory has been useful in understanding many aspects of granular matter [2–4], but its applicability is limited because in many situations the impact between grains is such that energy dissipating phenomena become relevant. Such phenomena, involving, for example, elastoplastic and viscoelastic behavior [5], are so complex that it is hard to think of a closed form force law that may describe them all at once.

However, energy loss can be measured experimentally, at the macroscopic level, by measuring the coefficient of restitution, which has been observed to decrease with the normal component of the relative impact velocity [6]. In this case, Hertz theory fails to reproduce the behavior of the coefficient of restitution. In [7,8], the authors have developed a quasistatic approximation to calculate the normal force acting between colliding particles, assuming a viscoelastic force (see also [9] where this force law appears in a related context, and [10] for a first-principles derivation of the viscoelastic term). Within this approach, where the force acting between beads is a combination of Hertz and viscoelastic terms, theory and experiment agree for the behavior of the coefficient of restitution with velocity [11].

In this Letter, a model that combines Hertz theory, a viscoelastic force as in [7,8], and a force proportional to the square of the relative velocities of beads is presented. It is shown that this model reproduces in an excellent way the effect of dissipation on a solitary wave in stainless steel, brass, and polytetraflouroethylene (PTFE) obtained by Daraio *et al.* [12]. It also coincides very well with the behavior of solitary wave trains in a column of stainless steel beads [13] and with the description of incident and reflected solitary waves in a column of PTFE balls [14]. To simulate such systems, I follow as closely as possible the experimental setup, including the reduction by less than 5.5% in mass of beads with inserted piezosensors.

Let $x_i(t)$ represent the displacement of the center of the ith sphere, of mass m_i, from its initial equilibrium position. The equations of motion that describe the dynamics of N beads, inclined by an angle α, in a gravitational field are

$$\begin{aligned} m_i\ddot{x}_i = {} & K_{i-1,i}\delta_{i-1}^{3/2} - K_{i,i+1}\delta_i^{3/2} + \frac{3A}{2}\{\sqrt{\delta_{i-1}}\dot{\delta}_{i-1} - \sqrt{\delta_i}\dot{\delta}_i\} \\ & + B\{\theta_{i-1}(\mathrm{sgn}[\dot{\delta}_{i-1}]\dot{\delta}_{i-1})^2 - \theta_i \mathrm{sgn}[\dot{\delta}_i]\dot{\delta}_i^2\} \\ & + m_i g \sin[\alpha], \end{aligned} \tag{1}$$

with $i = 2, \ldots, N-1$. As known, the equations of motion for the first and last beads differ from Eq. (1) and are thus not written down here. The notation is as follows: $\dot{\delta}_i = \dot{x}_i - \dot{x}_{i+1}$ is the relative velocity of beads i and $i+1$. The overlap between adjacent beads is $\delta_i = \max\{\Delta_{i,i+1} - (x_{i+1} - x_i), 0\}$, ensuring that the spheres interact only when in contact. For the same reason a step function in the third term has been included, that is, $\theta_i = \theta[\Delta_{i,i+1} - (x_{i+1} - x_i)]$. $\Delta_{i,i+1} = (g \sin[\alpha] i m_i / K_{i,i+1})^{2/3}$ appears from the precompression due to the gravitational interaction. The expression for the Hertz coupling $K_{i,j}$ between beads i and j is well known and depends on radii, Young moduli, and Poisson ratio of beads [5]. Although the form of parameter A is known for a binary collision [8], it is used here as a free parameter, like B itself. The set of Eqs. (1) is solved by using an explicit Runge-Kutta method of the 5th order with an embedded error estimator, from MATHEMATICA.

Our explanation for our ansatz is as follows: after the impact, the dynamics becomes a multi-impact problem; this produces that the relative velocity of beads i and $i+1$, $\dot{\delta}_i$, may change from $\dot{\delta}_i < 0$, related to an expansion phase,

to $\dot{\delta}_i > 0$, corresponding to a compressional phase. The same happens for the relative velocity of beads $i-1$ and i, $\dot{\delta}_{i-1}$. Therefore, by fixing our attention on one bead in the chain, say ith, one has a particle between two moving walls (beads i and $i+1$) and then its dynamics depends on the dynamics of both constraints. It is worthwhile to mention that a term proportional to the square of the velocity was introduced by Pöschl [15] as an attempt to extend the Hertz theory to plastic bodies. Also notice that if beads $i-1$, i and $i+1$ are all in contact at a given instant, one can easily observe that the third term can be generically written as

$$\dot{x}_{i-1}^2 + 2\epsilon\dot{x}_i^2 + \kappa\dot{x}_{i+1}^2 + 2\eta\dot{x}_i(\dot{x}_{i-1} - \sigma\dot{x}_{i+1}), \quad (2)$$

where the constants take the values $\epsilon = 0, 1$, $\kappa = \pm 1$, $\eta = \pm 1$, $\sigma = \pm 1$, depending on the sign of the relative velocities $\dot{\delta}_i$ and $\dot{\delta}_{i-1}$. Observe that the force term included in this Letter is a combination of two terms, only one of them being dissipative [16].

In Ref. [12], the effect of dissipation on the behavior of solitary waves was clearly shown. Beads made of stainless steel, brass, and PTFE, and a wall of aluminum were used in the experiment. Their Young modulus and Poisson ratio are (i) stainless steel: $E = 193 \times 10^9$ Pa; $\nu = 0.30$; (ii) brass: $E = 115 \times 10^9$ Pa; $\nu = 0.31$; (iii) PTFE: $E = 1.46 \times 10^9$ Pa; $\nu = 0.46$; and (iv) aluminum: $E = 69 \times 10^9$ Pa; $\nu = 0.33$. Strikers with the same mechanical properties as beads were used to generate solitary waves; the force on piezosensors was recorded, and the data presented as plots of force as a function of time.

In Fig. 1, the numerical findings from our model are compared with those shown in Fig. 1(b) of Ref. [12], that is, for a chain composed of $N = 70$ stainless steel beads, and impactor velocity $v_1 = 1.77$ m/s. Sensors are placed in beads 9, 16, 24, 31, 40, 50, 56, and 63. A *global* time shift of 25 μs of the extracted data was necessary in order to compare our findings with the experimental data from Fig. 1(b) of Ref. [12]. This shift possibly can be ascribed to an experimental time offset. Also, in the data received by the author, sensors appear in pairs, say sensors 2 and 4 (e.g., beads 16 and 31 for stainless steel). Thus, in order to compare this experimental data with the simulation, the original experimental data has been shifted such that the time interval between both maxima in the data is kept fixed, within an error of 0.2 μs. Thus, this shift does not represent a change in the time of flight, lying within the experimental errors. Figure 1 also shows, as an inset, the percentage error between experiment and simulation. One observes that this error is below 20% for the maximum amplitude, getting worse when approaching the wings of the signal, which is not surprising from the experimental point of view. Figure 2 shows a detail of Fig. 1, using original data, for the force recorded at beads 16 and 56. As one can see, the agreement between simulations and experiment is quite impressive. One possible combination of values of the parameters, not necessarily the optimal one, that gives a quite remarkable coincidence with experiment is $A = 800$ and $B = -1.9$.

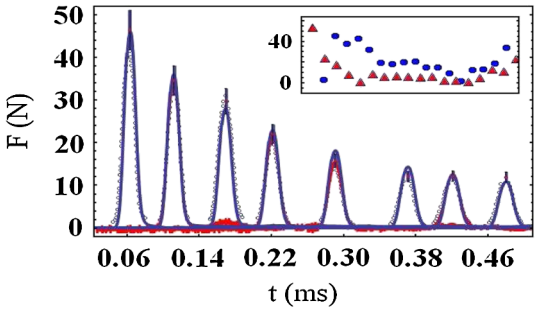

FIG. 1 (color online). The continuous curve shows our numerical findings. Open circles and error bars are experimental data extracted from Fig. 1(b) of Ref. [12]. The experimental outcome from sensors 16, 31, 40, and 56 is also shown. The inset shows the percentage error between experiment and simulation for beads 16 (triangles) and 40 (circles).

In Fig. 3, a striker with initial velocity $v_1 = 1.55$ m/s impacts on a chain of $N = 69$ PTFE beads and a chain of $N = 61$ brass spheres. Forces are recorded by sensors at beads 38 and 49, respectively. The numerical values of the parameters that caused theory and experiment to coincide are $A = 100$ and $B = -0.26$, for PTFE, and $A = 770$ and $B = -2.9$, for brass.

In the following, the simulation findings from our model are compared with those from experiments carried out by Nesterenko *et al.* with a column of PTFE beads [14] lying on a wall made of brass. There, solitary waves were generated by impacting the column of 21 beads, each with radius 2.38 mm and mass 0.123 g, with a PTFE ball with the same characteristics and with a 2.0 m/s impact velocity, the mechanical properties of materials being the same as above. In Figs. 4(a) and 4(b), there appear the incident and reflected perturbations recorded at positions 12 and 16, respectively, while Fig. 4(c) shows the behavior of the solitary wave at the wall. Because of the lack of detailed experimental information, global time shifts by 26 μs and 38 μs where applied to get coinciding incident perturbations in Figs. 4(a) and 4(b), respectively, while for Fig. 4(c), the shift made was 31 μs. Observe that the

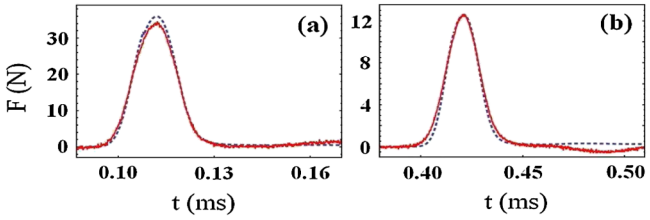

FIG. 2 (color online). The figure shows the force as a function of time for beads (a) 16 and (b) 56 for stainless steel. Dashed lines correspond to the numerical results.

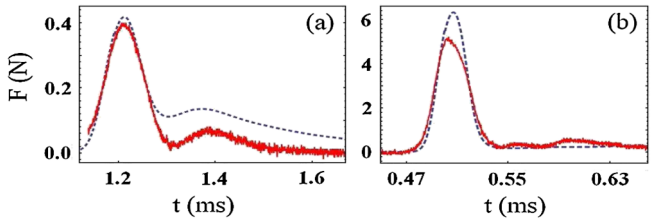

FIG. 3 (color online). Plots showing force as a function of time, for an impact velocity of $v_1 = 1.55$ m/s, for (a) PTFE (bead 38), and (b) brass (bead 49).

simulation fits quite well the experimental data. The same numerical values for the parameters of the model in case of PTFE are used, i.e., $A = 100$ and $B = -0.26$.

To end the tests on the validity of the model, the simulation results are compared with the outcomes from experiments carried out by Nesterenko *et al.* with a column of stainless steel beads [13]. The data, extracted from their paper, are used to show that the model reported here successfully describes the behavior of highly nonlinear waves on hard walls. In order to create the nonlinear waves, a column of 21 stainless steel beads, each with a mass 0.45 g, was struck by a cylindric alumina impactor, with Young modulus $E = 416 \times 10^9$ Pa and Poisson ratio $\nu = 0.23$. The cylinder has a mass 1.2 g and a velocity equal to 0.44 m/s. The force is recorded by embedding piezosensor in beads 12 and 16 (measured from the top of the column), and at the wall; the piezogauge at the wall was covered by a brass cover plate. As expected, because the impactor's mass is much larger than the mass of beads, trains of highly nonlinear solitary waves are excited by the impact. Figure 5 shows an excellent agreement between model and experiment; it must be stressed that the numerical values for the parameters are the same as before: $A =$

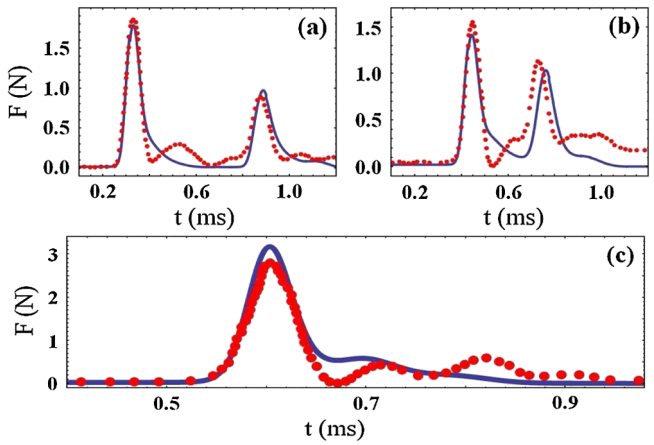

FIG. 4 (color online). Scattering of highly nonlinear waves off a wall for PTFE beads at positions: (a) 12 and (b) 16. In (c) the sensor is at the wall. Dots represent experimental data and the solid line the numerical output.

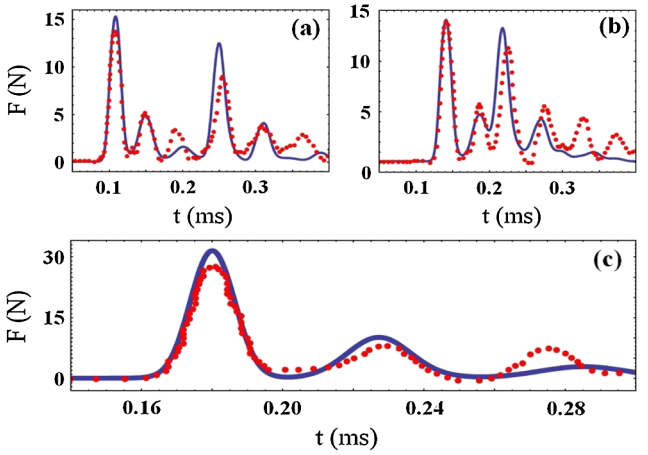

FIG. 5 (color online). Scattering of highly nonlinear waves off a wall for stainless steel beads at positions: (a) 12 and (b) 16. In (c) the sensor is at the wall. Data are shown as dots and numerical results as a solid line.

800 and $B = -1.9$. In order to compare experiment and simulation, the data were shifted 47 μs for Figs. 5(a) and 5(b), 45 μs for Fig. 5(c). The small time difference, of the order 7 μs, between the pulse amplitudes from the simulation and the experiments observed in Figs. 4, 5(a), and 5(b) can be ascribed to the combined properties of both wall and piezosensor. If a softer wall is assumed, the time difference and the amplitude of the reflected wave (and the force at the wall) can be reduced.

Finally, I compare the contribution of the viscoelastic and velocity-squared terms, using the force on bead 10. The Hertz interaction is by far the leading term and it is not included here. In Fig. 6, the force on bead 10 is plotted against time; time units are not made explicit because not

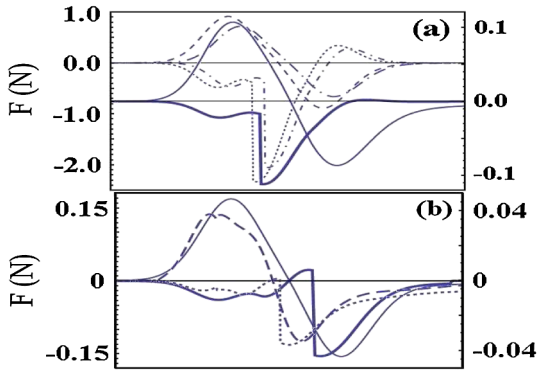

FIG. 6 (color online). (a) shows viscoelastic (1) and velocity-squared (2) forces as a function of time on bead 10, for beads of stainless steel [dashed (1) and dotted (2) lines], brass [long (1) and short (2) dot-dashed] and PTFE [thin (1) and thick (2) continuous], with the conditions of Figs. 1–3. (b) shows the force terms in case of reflected waves, using the data used in Figs. 4 and 5, for stainless steel [thin (1) and thick (2) continuous] and PTFE [dashed (1) and (2) dotted].

all of the plots correspond to the same time interval. Also, in Figs. 6(a) and 6(b) force values at the right-hand side correspond to PTFE. In Fig. 6(a), one observes that both terms give a contribution of the same order, but in some time intervals each acts in opposition to the other. A slightly different situation appears in the case of the reflected perturbations, as seen in Fig. 6(b). In this case, there is a time interval where both force terms reinforce their contribution. Also observe that the velocity-squared force term is a continuous, although not smooth, function of time. Nevertheless, this is not crucial for reproducing the experimental data.

In conclusion, a model that reproduces experimental outcomes for the behavior of highly nonlinear dissipative waves, for different materials and under different conditions, in one-dimensional dry granular media has been found. Excellent qualitative and quantitative agreement between theory and experiments is found, within the experimental errors of measurements of either force amplitude or time of flight, mostly depending on the Hertz interaction. The force term added in this Letter, proportional to the square of the relative velocity of particles, completes a previous physical model composed of Hertz and viscoelastic interactions which, without this term, is unable to reproduce experimental outcomes for the behavior of dissipative highly nonlinear waves. The new force term originates from multiple impacts within the system and is composed of two parts, one of which is dissipative. The model is economical, requiring only two parameters that depend on the mechanical properties of beads, one of them being well known and with clear physical origin. In addition, the parameter values do not need to be changed in order to fit simulations with experiments carried out under different conditions, and are found through a single fit procedure. Of course, if one is looking for the optimal set of parameters, one should perform a more complete analysis, like the one done in [12]. The model is, of course, not universally valid and, for example, is useless for describing the generation of oscillatory shock waves in soft materials as PTFE.

The author is indebted to Professor C. Daraio for discussions, for giving details about the experimental setup of Ref. [12], and for kindly providing most of the data shown in Figs. 1–3. Useful discussions, criticisms, and insight about experimental matters are deeply acknowledged to Professor R. Labbé. Useful suggestions and constructive criticism are acknowledged to Professor S. Fauve. This work was partially supported by Fondecyt, Grant No. 1085043.

*lautaro.vergara@usach.cl

[1] H. Hertz, J. Reine Angew. Math. **92**, 156 (1881).
[2] H. M. Jaeger and S. R. Nagel, Science **255**, 1523 (1992); *Physics of Dry Granular Media*, edited by H. J. Herrmann, J.-P. Hovi, and S. Luding, NATO Advanced Studies Institutes Series (Kluwer, Dordrecht, 1998); *The Physics of Granular Media*, edited by H. Hinrichsen and D. Wolf (Wiley-VCH, Berlin, 2004); in *Proceedings of the International Conference on Powders and Grains 2005*, edited by R. García-Rojo, H. J. Herrmann, and S. McNamara (Taylor and Francis, London, 2005).
[3] V. F. Nesterenko, *Dynamics of Heterogeneous Materials* (Springer, New York, 2001); S. Sen, M. Manciu, and J. D. Wright, Phys. Rev. E **57**, 2386 (1998); E. J. Hinch and S. Saint-Jean, Proc. R. Soc. A **455**, 3201 (1999); Hascoet and H. J. Herrmann, Eur. Phys. J. B **14**, 183 (2000); M. Manciu, S. Sen, and A. J. Hurd, Physica (Amsterdam) **157D**, 226 (2001); S. Sen *et al.*, Phys. Rep. **462**, 21 (2008), and references therein.
[4] C. Coste, E. Falcon, and S. Fauve, Phys. Rev. E **56**, 6104 (1997).
[5] K. L. Johnson, *Contact Mechanics* (Cambridge University Press, London, 1992).
[6] W. Goldsmith, *Impact* (Edward Arnold Publ., London, 1960); R. Sondergaard, K. Chaney, and C. E. Brennen, J. Appl. Mech. **57**, 694 (1990).
[7] G. Kuwabara and K. Kono, Jpn. J. Appl. Phys. **26**, 1230 (1987).
[8] N. V. Brilliantov, F. Spahn, J.-M. Hertzsch, and T. Pöschel, Phys. Rev. E **53**, 5382 (1996).
[9] C. Zener, Phys. Rev. **59**, 669 (1941).
[10] W. A. M. Morgado and I. Oppenheim, Phys. Rev. E **55**, 1940 (1997).
[11] R. Ramirez, T. Pöschel, N. V. Brilliantov, and T. Schwager, Phys. Rev. E **60**, 4465 (1999).
[12] R. Carretero-González, D. Khatri, M. A. Porter, P. G. Kevrekidis, and C. Daraio, Phys. Rev. Lett. **102**, 024102 (2009).
[13] C. Daraio, V. F. Nesterenko, E. B. Herbold, and S. Jin, Phys. Rev. E **73**, 026610 (2006).
[14] C. Daraio, V. F. Nesterenko, E. B. Herbold, and S. Jin, Phys. Rev. E **72**, 016603 (2005).
[15] T. Pöschl, Z. Phys. **46**, 142 (1927).
[16] In the term to the right, $\mathrm{sgn}[\dot{\delta}_{i-1}]$ multiplies only the first term of $\dot{\delta}_{i-1}$, i.e., $\dot{x}_{i-1}$